Detecting changes in seasonal precipitation extremes using regional climate model projections: Implications for managing fluvial flood risk

H. J. Fowler[1] and R. L. Wilby[2]

Received 3 December 2008; revised 6 July 2009; accepted 22 September 2009; published 23 March 2010.

[1] There is growing evidence of coherent, global patterns of change in annual precipitation and runoff with high latitudes experiencing increases consistent with climate model projections. This paper describes a methodology for estimating detection times for changes in seasonal precipitation extremes. The approach is illustrated using changes in UK precipitation projected by the European Union PRUDENCE climate model ensemble. We show that because of high variability from year to year and confounding factors, detection of anthropogenic climate change at regional scales is not generally expected for decades to come. Overall, the earliest detection times were found for 10 day winter precipitation totals with 10 year return period in SW England. In this case, formal detection could be possible within a decade from now if the climate model projections are realized. The outlook for changes in summer flash flood risk is highly uncertain. Our analysis further demonstrates that existing precautionary allowances for climate change used for flood management may not be sufficiently robust in NE England and east Scotland. These findings imply that for certain types of flood mechanism, adaptation decisions might have to be taken in advance of formally detected changes in flood risk. This reinforces the case for long-term environmental monitoring and reporting of climate change indices at "sentinel" locations.

Citation: Fowler, H. J., and R. L. Wilby (2010), Detecting changes in seasonal precipitation extremes using regional climate model projections: Implications for managing fluvial flood risk, *Water Resour. Res.*, *46*, W03525, doi:10.1029/2008WR007636.

1. Introduction

[2] There is a widely held perception that flood risk has increased across Europe during the last decade [*European Environment Agency*, 2005]. Following the summer 2007 flooding, the UK Government announced increased annual budgets for flood risk management that will reach £800 million by 2010. Inevitably, higher spending on flood defense infrastructure prompts questions about *when* and *where* to prioritize the investment? Furthermore, the UK Government's 2008 Climate Change Act places a statutory requirement upon competent authorities to undertake risk assessments as part of their duty to adapt to climate change. The *Environment Agency* (*EA*) [2007] is already calling on key utilities and public services to take responsibility for "climate proofing" critical infrastructure, facilities and services.

[3] Evidence of human influences on the hydrosphere has been accumulating steadily over the last two decades [*Burke et al.*, 2006; *Hegerl et al.*, 2007; *Santer et al.*, 2007; *Tett et al.*, 2007; *Willett et al.*, 2007; *Wu et al.*, 2005]. However, with the possible exception of rainfall reductions over southwest Australia [*Timbal et al.*, 2006], *attribution* of rainfall trends to human influence is not yet possible below the scale of the global land area [*Lambert et al.*, 2004; *Zhang et al.*, 2007]. Nonetheless, changes in moderately extreme precipitation events are, in theory, more robustly detectable than changes in mean precipitation [*Frei and Schär*, 2001] because as precipitation increases (under the greater water holding capacity of a warmer atmosphere) a greater proportion is expected to fall as heavy and very heavy rainfall events [*Kharin and Zwiers*, 2000; *Wehner*, 2004; *Hegerl et al.*, 2004, 2006; *Katz*, 1999; *Pall et al.*, 2007; *Trenberth et al.*, 2003]. Disproportionate increases in heavy rainfall have been widely reported for the observed climate record [*Alexander et al.*, 2006; *Groisman et al.*, 2005] but rates of change and/or regional patterns of observed and simulated rainfall extremes showed little similarity in early studies [e.g., *Kiktev et al.*, 2003]. This is partly due to the inability of climate models to adequately resolve extreme precipitation at subgrid box scales other than for winter [*Fowler et al.*, 2007; *Fowler and Ekström*, 2009]; the scale mismatch between point observations and gridded climate model output; and the difficulty of defining statistically robust "extreme" indices [*Hegerl et al.*, 2006].

[4] Even *detection* of hydrological change is far from straightforward because the choice of index, spatial and temporal scale of aggregation, statistical test (including significance testing), and confounding factors, all require careful consideration [*Kundzewicz and Robson*, 2004; *Radziejewski*

[1]Water Resource Systems Research Laboratory, School of Civil Engineering and Geosciences, Newcastle University, Newcastle upon Tyne, UK.
[2]Centre for Hydrological and Ecosystem Science, Department of Geography, Loughborough University, Loughborough, UK.

0043-1397/10/2008WR007636

and Kundzewicz, 2004; *Legates et al.*, 2005; *Svensson et al.*, 2005; *Wilby et al.*, 2010].

[5] 1. The chosen indicator might be monthly, seasonal, annual, rainfall/river flow, maxima, N day rainfall totals, proportional contributions, counts of peaks over threshold flows, point or area average data, individual records, pooled, or gridded data.

[6] 2. The period of record is important because when longer rainfall and river flow records are analyzed many trends found in shorter series cease to be significant. This can be due to the influence of outliers (at the start or the end of the record), or simply a result of multidecadal variability.

[7] 3. The power of statistical tests to detect change varies. Widely used methods include (logistic) linear regression, "change point" tests, and the nonparametric Spearman rank correlation and Mann-Kendall tests. Detectability of trends in extreme events can be improved through regional pooling of data.

[8] 4. Confounding factors such as creeping or sudden changes in meteorological records can arise from changes in site, instrumentation, observing or recording practices, site characteristics, or sampling regime. Discharge records may be biased by many nonclimatic influences including land cover and management, urbanization, river regulation, water abstraction and effluent returns, or flood flows bypassing gauging structures.

[9] The number of years of rainfall or runoff record needed to detect a statistically significant trend depends on: the strength of the trend; the amount of variance about the trend; the probability of erroneous detection (type 1 error); and the probability of missing a real trend (type 2 error). Preliminary estimates using data for river basins in the United States and United Kingdom suggest that statistically robust, climate-driven trends in *seasonal* runoff are unlikely to be found until the second half of the 21st century [*Ziegler et al.*, 2005; *Wilby*, 2006]. In Australian river basins an even greater change may be required for detection as the interannual variability of flows is twice that of Northern Hemisphere river basins [*Chiew and McMahon*, 1993].

[10] Detection time relationships can also be inverted to estimate the strength of trend required for detection by specified time horizons. For example, analysis of UK winter and annual precipitation totals suggests that changes of ~25% would be needed for detection by the 2020s in the most sensitive basins (such as the River Tyne). Although increases (or decreases) in seasonal totals could affect overall flood risk, it is suspected that more useful flood risk information can be extracted from daily precipitation indices. Furthermore, as noted before, projected trends in indices of heavy precipitation may be detectable earlier than trends in seasonal means [*Hegerl et al.*, 2004].

[11] Although attribution of changes in precipitation or flood risk is not feasible for individual basins, techniques have emerged for estimating the time horizons for formal detection at regional scales. This paper describes a methodology for estimating detection times for changes in seasonal precipitation extremes as projected by the European Union PRUDENCE (Prediction of Regional scenarios and Uncertainties for Defining European Climate change risks and Effects [*Christensen et al.*, 2007]) Regional Climate Model (RCM) ensemble. Changes in UK precipitation extremes are used as the test case. Section 2 provides a description of the RCM outputs and meteorological observations used in the study, and Section 3 details the methodology for trend detection in selected indices of extreme precipitation. Section 4 explores *when* and *where* changes in downscaled UK rainfall metrics are not likely to have been entirely the result of (model estimated or observed) natural variability. We also examine the extent to which existing precautionary allowances used for flood risk assessment are exceeded by the projected climate changes. Section 5 then discusses how the results might inform protocols for monitoring and adapting to changing flood risk, as well as topics for further research. A few concluding remarks are made in section 7.

2. Observed and Climate Model Precipitation Indices

[12] The methodology for detecting changes to extreme precipitation metrics relies on a combination of regional frequency analysis (RFA) and pattern scaling. The estimation of the frequencies of extreme events is difficult as extreme events are, by definition, rare and observational records are often short. In RFA, data from the "region" are assumed to share the same frequency distribution and only differ in their magnitude (mean or median values). Therefore, RFA trades "space for time" and pools standardized data from several different sites within a "region" to fit a single frequency distribution [*Hosking and Wallis*, 1997].

2.1. Model Outputs and Data

[13] We employed thirteen RCM integrations from the PRUDENCE ensemble. All experiments yield daily precipitation totals for control (1961–1990) and future (2071–2100) time periods [*Christensen et al.*, 2007] under the IPCC SRES A2 emissions scenario [*Nakićenović et al.*, 2000] (Table 1). Nine of these RCM experiments were conducted by nesting within the atmosphere-only high-resolution General Circulation Model (GCM) HadAM3H of the UK Hadley Centre. One RCM, HadRM3P, was nested within HadAM3P, a more recent version of the same atmosphere-only GCM; but HadRM3H and HadRM3P can be considered as essentially the same model for Europe [*Moberg and Jones*, 2004]. The variable resolution global atmospheric model, Arpége, is nested directly within HadCM3. Additionally, two RCM integrations, HIRHAM and RCAO, are driven by lateral boundary conditions from two separate integrations of the ECHAM4/OPYC3 coupled ocean-atmosphere GCM (see http://prudence.dmi.dk/public/DDC/extended_table.html).

[14] All the RCMs operate with grid spacing of ~0.5° longitude by ~0.5° latitude (~50 km spatial resolution) over a European domain and data were regridded to a regular 0.5° × 0.5° grid using an inverse distance weighted interpolation algorithm to allow direct comparison between models (Figure 1). More details of the experimental design of the PRUDENCE integrations can be found in *Jacob et al.* [2007].

[15] An observational precipitation data set at a comparable scale to the RCM outputs was produced by taking a daily average across the 5 km boxes contained within each 0.5° × 0.5° grid cell for each day of 1958–2002 for the UK Meteorological Office data set [*Perry and Hollis*, 2005a, 2005b].

Table 1. Eleven Regional Climate Models and 13 Integrations From the PRUDENCE Ensemble Used in This Study[a]

Acronym	Institution/Model Origin and References	RCM	GCM
ARPH	French Meteorological Service; ARPEGE/IFS variable resolution global model. Model from *Déqué et al.* [1998].	Arpège	HadCM3
HADH	Hadley Centre, UK Meteorological Office, Exeter; Regional model at the Hadley Centre. Model from *Jones et al.* [2004a]	HadRM3P	HadAM3P
HIRH	Danish Meteorological Institute, Copenhagen; Dynamical core from HIRLAM, Parameterizations from ECHAM4. Model from *Christensen et al.* [1996, 1998]. Physiographic data sets from *Hagemann et al.* [2001] and *Christensen et al.* [2001].	HIRHAM	HadAM3H
HIRE	Danish Meteorological Institute, Copenhagen; Dynamical core from HIRLAM, Parameterizations from ECHAM4. Model from *Christensen et al.* [1996, 1998]. Physiographic data sets from *Hagemann et al.* [2001] and *Christensen et al.* [2001].	HIRHAM	ECHAM4/OPYC
RCAOH	Swedish Meteorological and Hydrological Institute, Stockholm; Rossby Centre Atmosphere Ocean Model. Model from *Jones et al.* [2004b], *Meier et al.* [2003], *Döscher et al.* [2002], and *Räisänen et al.* [2004].	RCAO	HadAM3H
RCAOE	Swedish Meteorological and Hydrological Institute, Stockholm; Rossby Centre Atmosphere Ocean Model. Model from *Jones et al.* [2004b], *Meier et al.* [2003], *Döscher et al.* [2002], and *Räisänen et al.* [2004].	RCAO	ECHAM4/OPYC
CHRMH	Swiss Federal Institute of Technology (ETH), Zurich; Climate High-Resolution Model. Model from *Lüthi et al.* [1996] and *Vidale et al.* [2003].	CHRM	HadAM3H
CLMH	GKSS, Institute for Coastal Research, Geesthatcht, Germany; Climate version of "Lokalmodell" of German Weather Service. Model from *Steppeler et al.* [2003].	CLM	HadAM3H
REMOH	Max Planck Institute for Meteorology, Hamburg, Germany; Dynamical core from "Europamodell" of German Weather Service, Parameterizations from ECHAM4. Model from *Jacob* [2001] and *Roeckner et al.* [1996].	REMO	HadAM3H
PROMH	Universidad Complutense de Madrid, Spain; Climate version of PROMES model. Model from *Castro et al.* [1993] and *Arribas et al.* [2003].	PROMES	HadAM3H
REGH	The Abdus Salam International Centre for Theoretical Physics, Italy (ICTP); Dynamical core from MM5, Parameterizations from CCM3. Model from *Giorgi et al.* [1993a, 1993b] and *Pal et al.* [2000].	RegCM	HadAM3H
RACH	The Royal Netherlands Meteorological Institute (KNMI), Netherlands; Dynamical core from HIRLAM, Parameterizations from ECMWF physics. Model from *Tiedtke* [1989, 1993] and *Lenderink et al.* [2003].	RACMO2	HadAM3H
METH	Norwegian Meteorological Institute; Version of HIRHAM. Model from *Christensen et al.* [2001] and *Hanssen-Bauer et al.* [2003].	MetNo	HadAM3H

[a]The acronyms explain the format of each model run. The first part refers to the RCM, and the second part to the GCM supplying the boundary conditions. Suffixes E and H denote RCMs driven by ECHAM4/OPYC3 and HadAM3H/P/HadCM3 GCMs, respectively.

2.2. Extreme Precipitation Indices

[16] Seasonal maximum (SM) series of 1, 5 and 10 day (henceforth 1d, 5d and 10d) precipitation totals are extracted for each grid cell, i, for each RCM time-slice (the control period, 1961–1990, and future period, 2071–2100), and for observations. These SM series were standardized by their median ($Rmed_i$, which is equivalent to the 2 year return value [after *Fowler et al.*, 2005]) to remove grid cell–specific factors from the regional analysis and to allow the regional pooling of standardized data for each of the nine UK rainfall regions delineated by *Wigley et al.* [1984] (Figure 1). The homogeneity of these regions for extreme precipitation was previously confirmed by *Fowler and Kilsby* [2003a]. A Generalized Extreme Value (GEV) distribution was fitted to each pooled standardized SM sample using Maximum Likelihood Estimation (MLE) and return values of precipitation intensities with average recurrence of 10 and 50 years were estimated (henceforth 10y and 50y). The estimates were then rescaled using the regional average Rmed from the appropriate original SM data set. Full mathematical details of the regional frequency analysis (RFA) are provided in Appendix A.

[17] A further step is needed to estimate transient changes in the return values of precipitation intensities for each RCM between the two time slices, 1961–1990 and 2071–2100. We applied a conventional pattern scaling approach [*Mitchell*, 2003]. The technique assumes that regional changes in

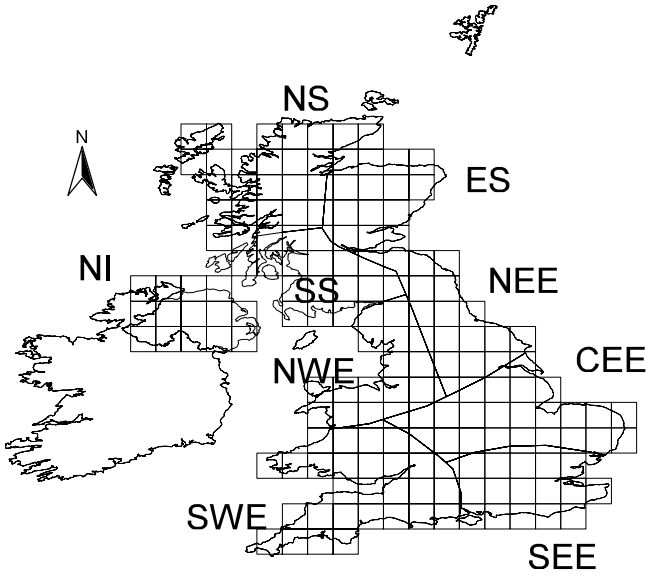

Figure 1. The RCM regular 0.5° by 0.5° grid and the nine coherent rainfall regions of the United Kingdom: North Scotland (NS), East Scotland (ES), South Scotland (SS), Northern Ireland (NI), Northwest England (NWE), Northeast England (NEE), Central and Eastern England (CEE), Southeast England (SEE), and Southwest England (SWE) [from *Fowler et al.*, 2007].

extreme precipitation (or any climate variable) will occur in proportion to the projected change in global mean temperature, in this case, from the two GCMs providing lateral boundary conditions for the 13 PRUDENCE RCMs (i.e., HadCM3 and ECHAM4). Pattern scaling was based on the change in global mean temperature predicted for 30 year time slices centered on the years 1975, 2025, 2055 and 2085. Therefore, designating the global mean temperature as T_y where y is the central year (1975, 2025, 2055 and 2085), the scale factor for each GCM time slice is given by

$$SF_y = \frac{T_y - T_{Con}}{T_{Fut} - T_{Con}}, \quad (1)$$

where T_{Con} and T_{Fut} indicate the global mean temperature for the Control (1961–1990) and Future (2071–2100) time slices, respectively. For intervening years the scale factors were linearly interpolated to provide transient scale factors. Therefore, for 1975 to 2085, *SF* varies from zero to one. The transient scale factors reflect the expected acceleration of global mean temperature changes over the next 100 years. An alternative to pattern scaling on global mean temperature change would be to simply apply linear scaling between 1990 and 2100; this would imply earlier detection times. We use the more conservative nonlinear pattern scaling to estimate return values of precipitation intensities and the associated confidence intervals for each year between 1990 and 2100.

3. Method for Detecting Change to Extreme Precipitation

[18] We define a detectable increase in extreme precipitation, D_x, as the point (year) at which we would reject (at the $\alpha = 0.05$ or 95% significance level) the null hypothesis that the return level estimated for the 1961–1990 period, μ_c, and the return level estimated for a year x (where $x > 1990$), μ_x, are equal in favor of the alternative hypothesis that μ_x is not equal to μ_c. This statistical test is based on the signal-to-noise ratio and provides a distribution that is approximately normally distributed with a mean of zero and a standard deviation of 1; $N(0,1)$ (see equation (1)). We then use a two-tailed Student's t test (assuming that the trend can go down as well as up) to estimate the point at which the return levels are shown to be from a significantly different population at the $\alpha = 0.05$ level, i.e., where $D_x \geq 1.96$:

$$D_x = \frac{|\mu_x - \mu_c|}{\sqrt{\sigma_f^2 + \sigma_c^2}} \geq 1.96, \quad (2)$$

where μ_x is the pattern-scaled return level for year x, μ_c is the estimated return level for the control period (1961–1990), σ_f^2 is the variance in the return level estimate for the RCM generated future period (2071–2100) and σ_c^2 is the variance in the return level estimate for the RCM generated control period (1961–1990). Note that the observed variance, $2\sigma_o^2$, for both 1961–1990 and 1958–2002 was substituted for the summed variance from the RCM control and future integrations, $\sigma_f^2 + \sigma_c^2$, in equation (2), to establish the sensitivity of the test to assumed variance (where the delta confidence intervals on the return level estimates were also calculated using the same assumed variance estimate, either RCM generated or observed for 1961–1990 and 1958–2002, respectively, as previously stated). This test defines the "detection year," D_x, as the first year at which $D_x \geq 1.96$ (the transient return level estimate for year x is significantly different to the return level estimate for the control period (1961–1990) at the $\alpha = 0.05$ level).

[19] We apply the principle of equal weighting across different RCMs to produce probability distributions of estimated D_x for change to the return levels of seasonal extreme precipitation in the nine UK rainfall regions. This is because extremes in winter are to a large extent determined by the boundary conditions imposed on the RCM. Since most RCMs in the PRUDENCE ensemble are driven by the same GCM (HadCM3), weighting model results based on observed extremes generally has a small impact [*Fowler and Ekström*, 2009; *Manning et al.*, 2009]. However, we did examine the sensitivity of D_x to the assumed variance in extremes and to the α level used in the detection test. The analysis is truncated at 2100 as we cannot assume that the pattern scaling relationship holds true after this time. Furthermore, although the analysis includes summer precipitation extremes, it should be noted that the present generation of RCMs do not adequately reproduce observed extremes during this season [*Fowler and Ekström*, 2009]. Throughout the study we define the point beyond which the probability of detection is more likely than not as when more than 50% of the RCMs detect a significant change in extreme precipitation.

4. Results

4.1. Estimated Changes to Seasonal Extreme Precipitation by the 2020s, 2050s, and 2080s

[20] Before estimating the detection times, it is useful to consider the changes in seasonal extreme precipitation projected by the RCM ensemble as larger changes, in general, imply earlier detection times.

[21] Box and whisker plots show the mean and uncertainty in changes to extreme precipitation by the 2020s, 2050s and 2080s for each region and season as projected by the RCM ensemble (Figures 2 and 3). Figures 2a and 2b show projected changes in the 1d10y and 10d10y totals in winter. Figures 3a, 3b, and 3c show projected changes to the 1d10y totals in spring, summer and autumn, respectively. For material on other precipitation totals and return periods, see auxiliary material.[1] The seasonal results for the 2080s are similar to those detailed by *Fowler and Ekström* [2009] for their equal weighting example. Additionally, *Fowler et al.* [2007] provide results for a subset of six of the 13 RCMs for percentage change to annual extreme precipitation by the 2080s. Notable increases in the magnitude of both short- and long-duration extreme precipitation events are projected for all seasons where climate model simulations adequately represent observed extreme precipitation (winter, spring and autumn [see *Fowler and Ekström*, 2009]). There is, however, uncertainty in the absolute magnitude as individual RCM projections differ.

[22] Winter 1d totals are projected to increase in all regions (Figure 2a). At the 10y return level, RCM ensemble projections for all regions, except for SEE, are positive; changes upward of 20% are projected for some regions by the most extreme RCMs by the 2050s (Figure 2a). There is more uncertainty at higher return levels with projected

[1] Auxiliary materials are available in the HTML. doi:10.1029/2008WR007636.

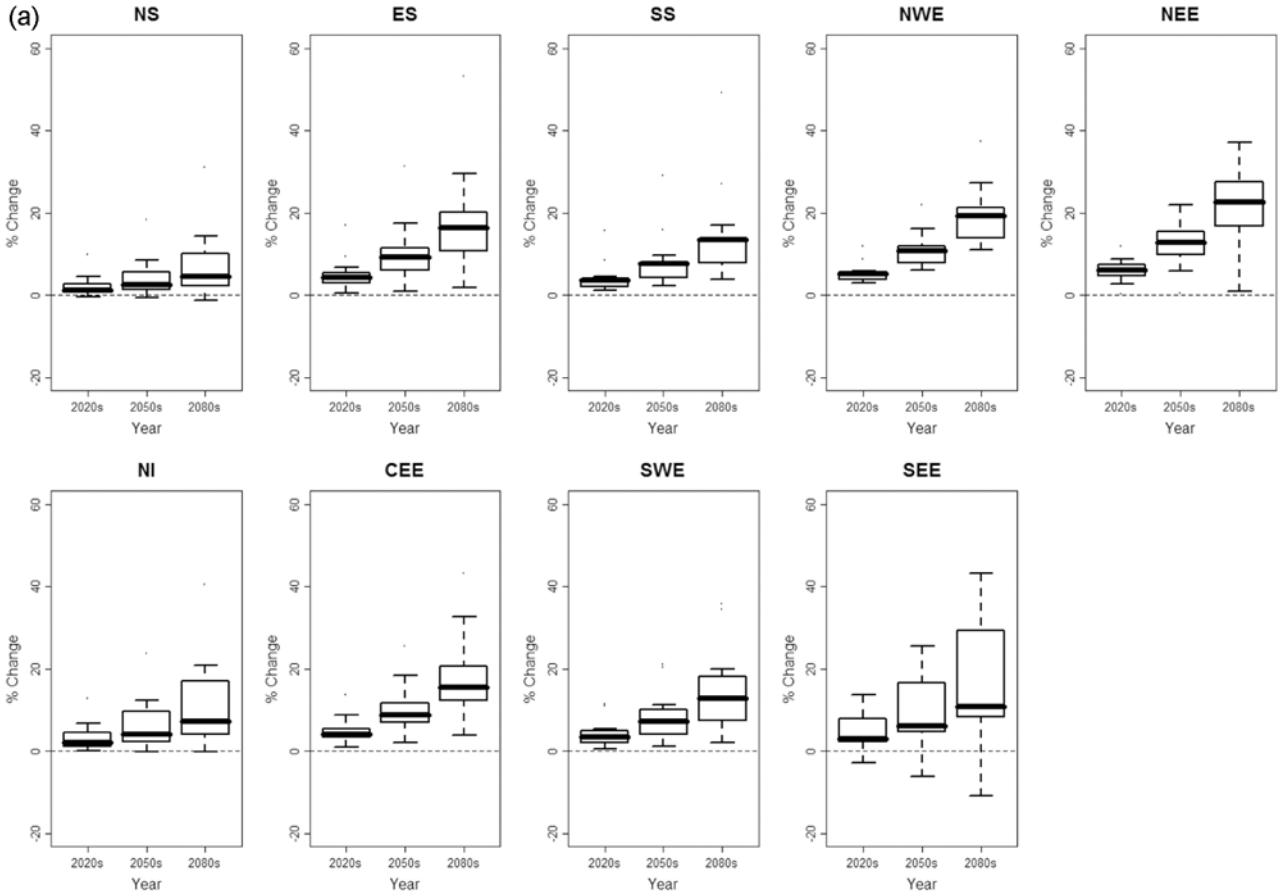

Figure 2. Box and whisker plots showing the mean and uncertainty in percentage changes to precipitation by the 2020s, 2050s, and 2080s projected by the PRUDENCE RCMs for winter (a) 1d10y and (b) 10d10y totals.

changes to the winter 50y return level showing a larger range of possible change; generally positive in the northern United Kingdom and negative in the southern United Kingdom (not shown). Winter 10d totals are also projected to increase in all regions at the 10y return level (Figure 2b), although the magnitude of these is overall smaller than for the 1d totals. Again, there is greater uncertainty in the projected changes to 10d50y totals, although these span the zero change line only in ES and NEE (not shown).

[23] In spring, increases in magnitude are projected for both the 1d10y and 10d10y totals. Changes approaching 20% are projected for the 1d10y totals by the 2080s for all of the northern United Kingdom, except for NS (Figure 3a), but changes to the 10d10y totals are smaller than this (not shown). There is greater uncertainty in projections of change to the 50y return level, but the potential for very large increases (up to 50%) in the 1d50y totals during spring by the 2080s (not shown).

[24] In summer, we have least confidence in climate model projections as reproduction of observed precipitation extremes by RCMs is poor [*Fowler and Ekström*, 2009]. This season has the largest uncertainty for all regions, return levels and daily aggregations (Figure 3b). Furthermore, the regridding of RCM output onto the coarser CRU grid (see section 2.1) would be expected to have most effect on the distribution of extremes in summer given the preponderance of more localized events during this season.

[25] In autumn, potentially very large percentage increases of up to 60% are projected for 1d50y totals by the 2080s (not shown), although uncertainties are large. For 1d10y totals, mean changes are all positive or the distribution is positively skewed with changes approaching 20% possible by the 2050s (Figure 3c). Projected changes to the magnitude of 10d totals are not as large as those projected for 1d totals (not shown); however, they are in the main positive and large changes are projected for 10d totals for northern regions at the 50y return level (not shown).

4.2. Detection Time Estimates and Sensitivity to Variance and Significance Level Estimates

[26] Empirical cumulative distribution functions (CDFs) of detection time by region and season were calculated for 1d and 10d precipitation totals and for 10y and 50y return levels. The detection time, D_x, is sensitive to (1) the assumed variance used to calculate confidence intervals on the return level estimates (95% delta confidence intervals are calculated in all cases) and in the detection test and (2) the α significance level used in testing "detectability" (note that the standard used is the $\alpha = 0.05$ level). Figure 4 shows an example of the detection times for significant change (at the

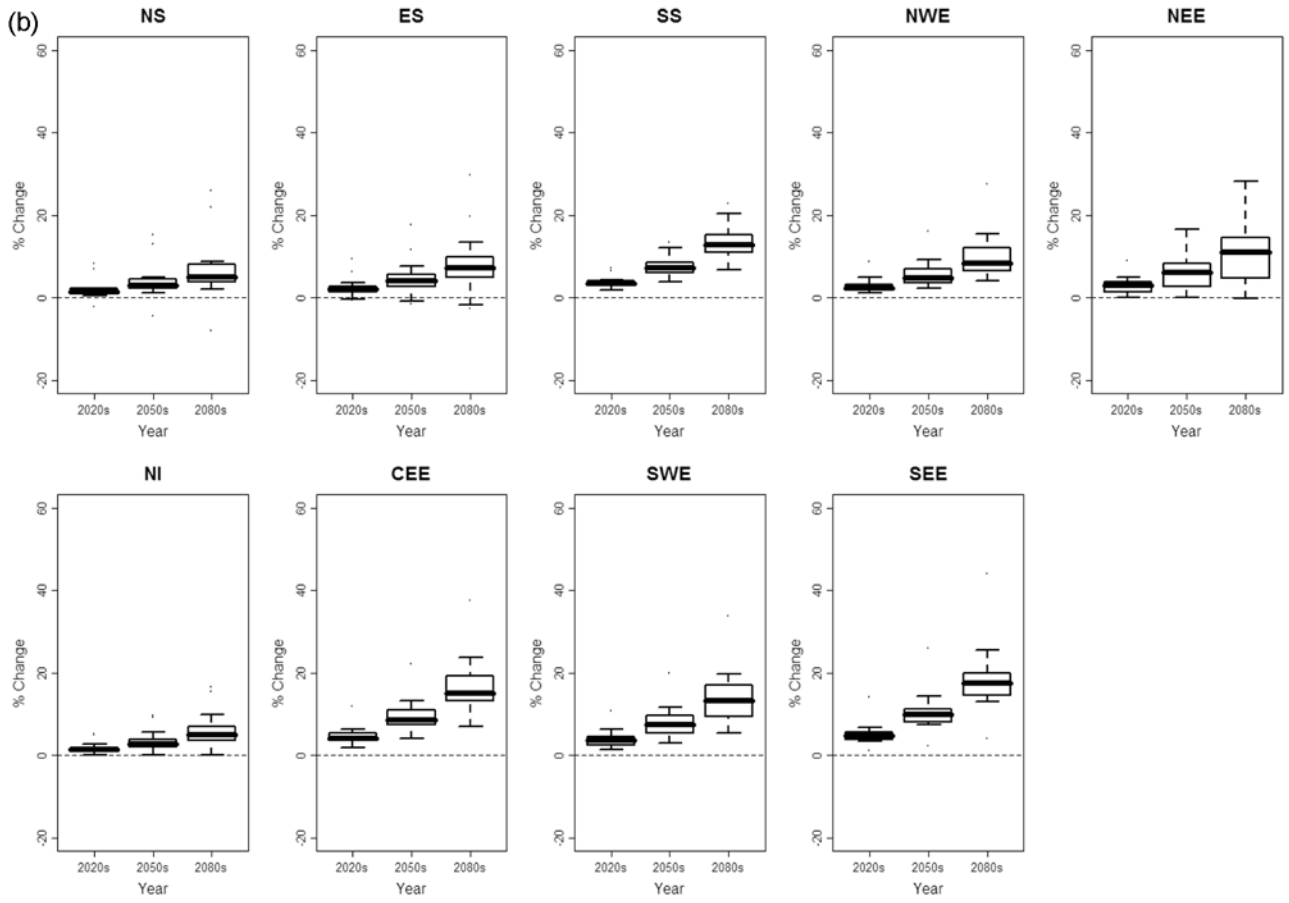

Figure 2. (continued)

α = 0.05 level) to winter 1d10y and 10d10y totals. In these plots, the vertical black dotted line indicates the year 2050 and the horizontal red dashed line the point beyond which the probability of detection is more likely than not. Three individual cumulative frequency distributions are shown on each plot. The green CDF shows the detection time, D_x, using RCM internal variability; the red CDF shows the same but for observed variability for 1961–1990; the black CDF shows the same but for the full record of observed variability from 1958 to 2002. Table 2 shows the year where the probability of detection is >0.5 for 1d and 10d winter precipitation totals, with 10y and 50y return levels and given the three different variance estimates for all regions. Although individual CDFs are not presented for the other seasons a summary of the earliest detection time and the season of earliest detectability for each region are given in Table 2 for completeness.

[27] Figure 5 shows the sensitivity of D_x to the α significance level used in testing "detectability" for all regions for a season where detectability is high (Figure 5a, winter) and detectability is lower (Figure 5b, spring). For each panel, the solid black line shows results for the 1d10y total; the dashed black line signifies the 1d50y total; the solid red line the 10d10y total; and the dashed red line the 10d50y total. The bold black vertical line in each panel shows the α = 0.05 level used in this study. Figure 5 confirms that as the α significance level increases (from 0.5 to 0.001) more observations are needed to detect a significant difference between the two sample populations and so the detection time is later.

[28] The summary in Table 2 and example in Figure 4 show that there are no consistent patterns (across all regions) of earlier or later detection time for the different variance estimates. On average, the RCM-estimated internal variability and observed variability for 1961–1990 yield longer detection times. For example, for the winter 1d10y total the mean detection time is 2045 for RCM-estimated variability, 2055 for observed variability based on 1961–1990, but 2042 when based on 1958–2002 (see Table 2). With only 30 years data, albeit with regional pooling, the confidence intervals on the return level are wide due to the relatively large uncertainty (variability) in the estimate. In general, use of the full record of observed variability available from the UK Meteorological Office 5 km gridded data set (for 1958–2002) provides the shortest detection times for both 1d and 10d totals. Occasionally, the RCM-estimated internal variability or the 1961–1990 observed variability yield shorter detection times, see for example the winter 10d10y total mean detection times in Table 2. In these cases, low variance of seasonal maxima within the

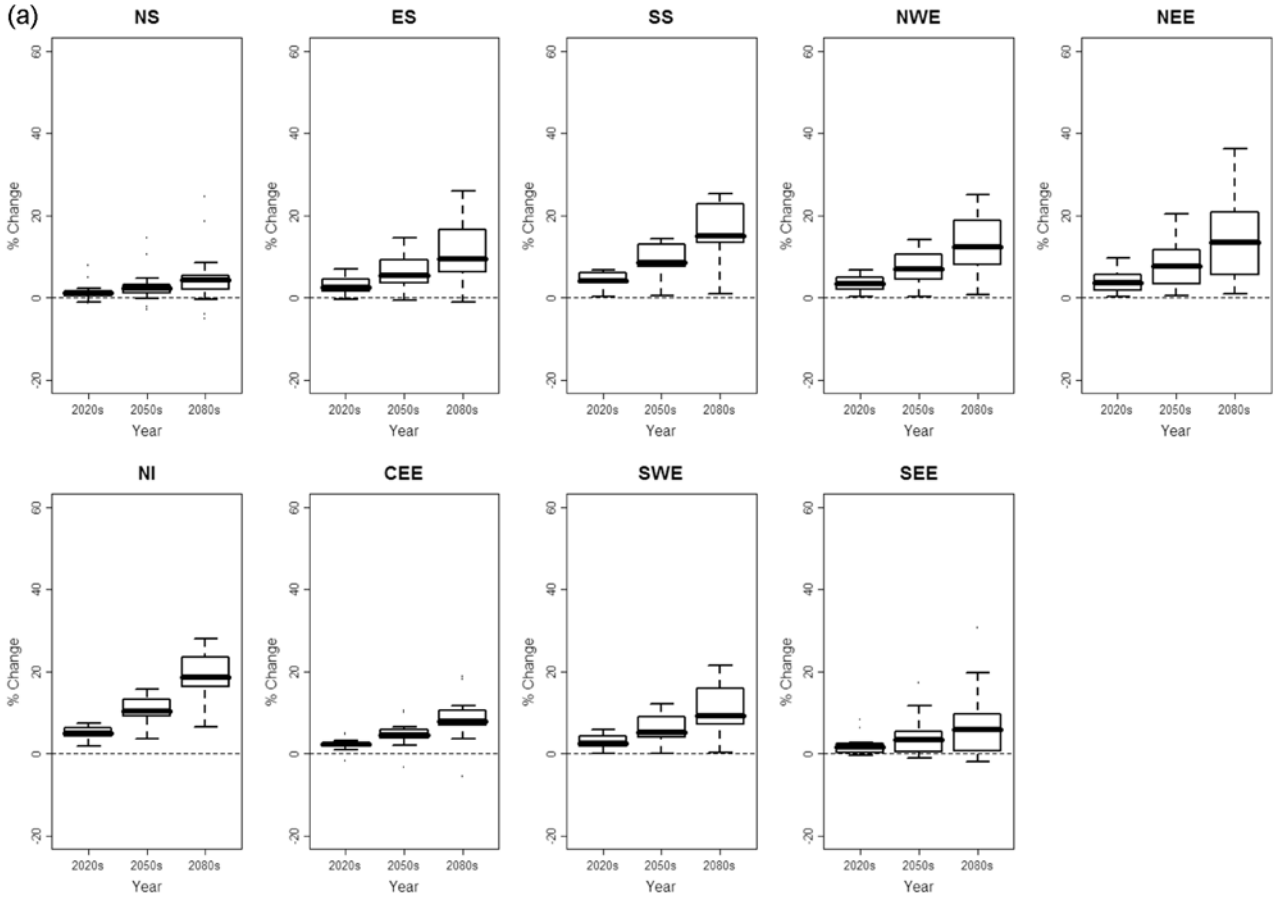

Figure 3. As in Figure 2 but for 1d10y precipitation totals in (a) spring, (b) summer, and (c) autumn.

RCM integration (and/or outliers in the longer observed record) decreases (increases) the width of confidence intervals and thus produces shorter (longer) detection times. However, earlier records prior to the early nineteenth century are thought to be less representative of the present climate regime [e.g., see *Marsh et al.*, 2007] and so were not used to characterize the variance statistic.

[29] Figure 4 and Table 2 show that for many UK regions, significant changes to extreme precipitation in winter are likely to be detectable by the 2050s, particularly for 1d totals. Detection times are, on average, earlier for higher frequency extreme precipitation events, i.e., those with shorter return period. For western and northern parts of the United Kingdom, it is likely that changes may be detectable even earlier, perhaps as soon as the 2020s. This is consistent with the large upward trends seen in observations of extreme precipitation in these regions since 1990 [*Fowler and Kilsby*, 2003a, 2003b]. It is perhaps surprising that changes to winter extreme precipitation are not likely to be detectable in North Scotland until 2080, given the observed positive trend in extreme precipitation reported for this region [*Fowler and Kilsby*, 2003a]. However, this may be explained by the large natural variability in winter precipitation amounts and, therefore, much wider confidence intervals calculated for this region. In both North and East Scotland the earliest detection times, ~2030s, are found for the autumn season (Table 2). Detection times for 10d50y precipitation totals are generally longer than for 1d50y totals (based on observed variability). However, detectability for 10d10y totals is higher than for 1d10y totals in winter for regions such as SW, SE and CE England (compare Figure 4a and Figure 4b). Overall, the earliest detection time is for 10d10y totals in winter in SW England, based on the RCM variance estimate. In this case, detection could be as early as 2016. Changes could also be detectable pre-2020 in 10d totals for SS.

[30] Detectability in other seasons is undoubtedly lower than in winter (see auxiliary material). In particular, in summer it is unlikely that changes will be detectable by 2050; for many regions, changes are not detectable by the end of the 21st century. In spring, for 1d10y and 10d10y totals it is likely that changes will detectable in most regions by 2080 but for longer return period events, for many regions and indices, detection is not achieved by the end of the 21st century. Detectability is greater in autumn than in spring and soonest in Scotland, where changes may be detectable by 2030 to 2050 for both 1d and 10d totals. Overall, the earliest detection time in spring was for the 1d10y event in NI (2033), and in autumn for the 1d10y event in SWE (2023).

[31] Figure 6 shows the minimum, mean and maximum year in which the probability of detection is more likely than not (i.e., more than 50% of the RCMs suggest that change is detectable by this year), for any season or detection index. It can be seen that detection is likely in all regions by 2060 to 2080 (the mean detection time using all statistics from all

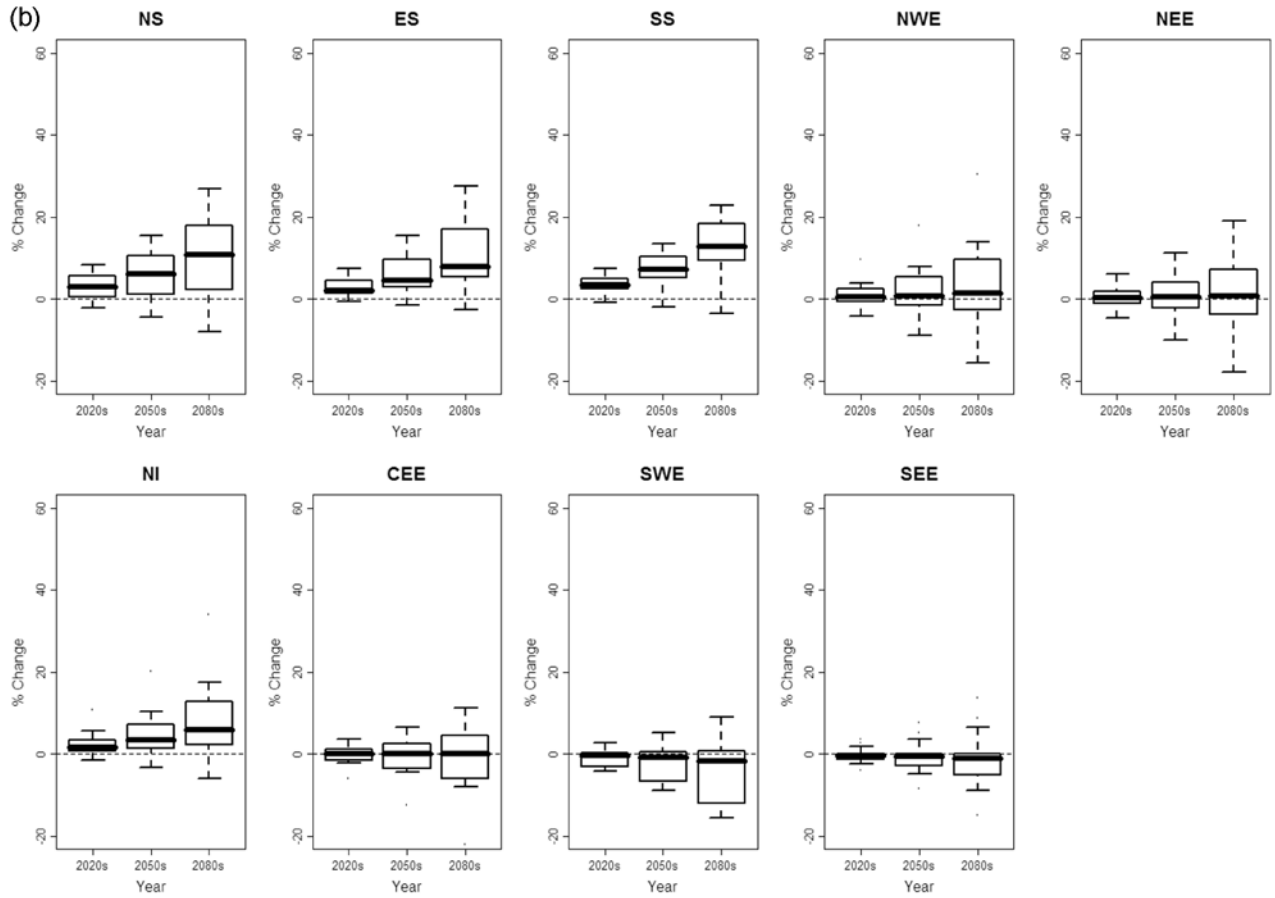

Figure 3. (continued)

seasons). However, detection is likely earlier than this for individual seasons and return levels. Note also that for some individual RCMs the detection year is pre-2020. The earliest detection time from any season, rainfall aggregation and return level is pre-2020 for SWE, and pre-2030 for all regions other than NI and ES where it is pre-2040 (refer also to the summary of earliest detection times at the bottom of Table 2).

4.3. Time Taken to Exceed Precautionary Allowance for Extreme Precipitation

[32] UK Planning Policy Statement 25 (PPS25) includes precautionary allowances for climate change for use in flood risk assessments [*Department of Communities and Local Government* (*DCLG*), 2006]. The *DCLG* [2006] and *Department of Environment, Food and Rural Affairs* (*DEFRA*) [2006] guidance applies to changes in peak rainfall intensity (cited in look-up tables as mm h^{-1} but with no accompanying return period) so the analysis of 1d totals here should be regarded only as indicative. The allowances were informed by *Ekström et al.* [2005] for changes to *annual* extreme precipitation and the +20% allowance (+30% in Scotland) applies to the period 2055–2085, with smaller allowances for earlier periods of +5% (1990–2025) and +10% (2025–2055).

[33] The PRUDENCE RCM scenarios provide scope for reviewing existing guidance and helping to refresh the UK climate change allowances used in flood risk management [*DCLG*, 2006; *DEFRA*, 2006]. For example, design standards for protection against storms and flooding by sewerage systems do not take into account climate change, but there is an "industry standard" of protection against a 1 in 30 year event [*Coulthard et al.*, 2007]. Others have questioned whether flood defenses based on the historic 1 in 100 year flood level provide an adequate standard of protection in the face of climate change [*Gloucestershire County Council* (*GCC*), 2007]. In some instances, conflicting policy goals are an impediment to coherent adaptation, for example the imperative to build more homes on brown field sites while at the same time avoiding high flood risk areas and catering for habitat migration. There is an implicit assumption that "people are becoming more at risk from all types of flooding because of climate change" [*EA*, 2007, p. 15] and that "as climate change makes extreme weather and flooding ever more likely, it is essential that public organizations and private companies act now to prevent major disruption and misery in the future" [*EA*, 2007, p. 48].

[34] We test when the +5% (1990–2025), +10% (2025–2055) and +20% (2055–2085) precipitation allowances in PPS25 could be exceeded, by estimating the minimum and mean year in which the probability of exceedance of the

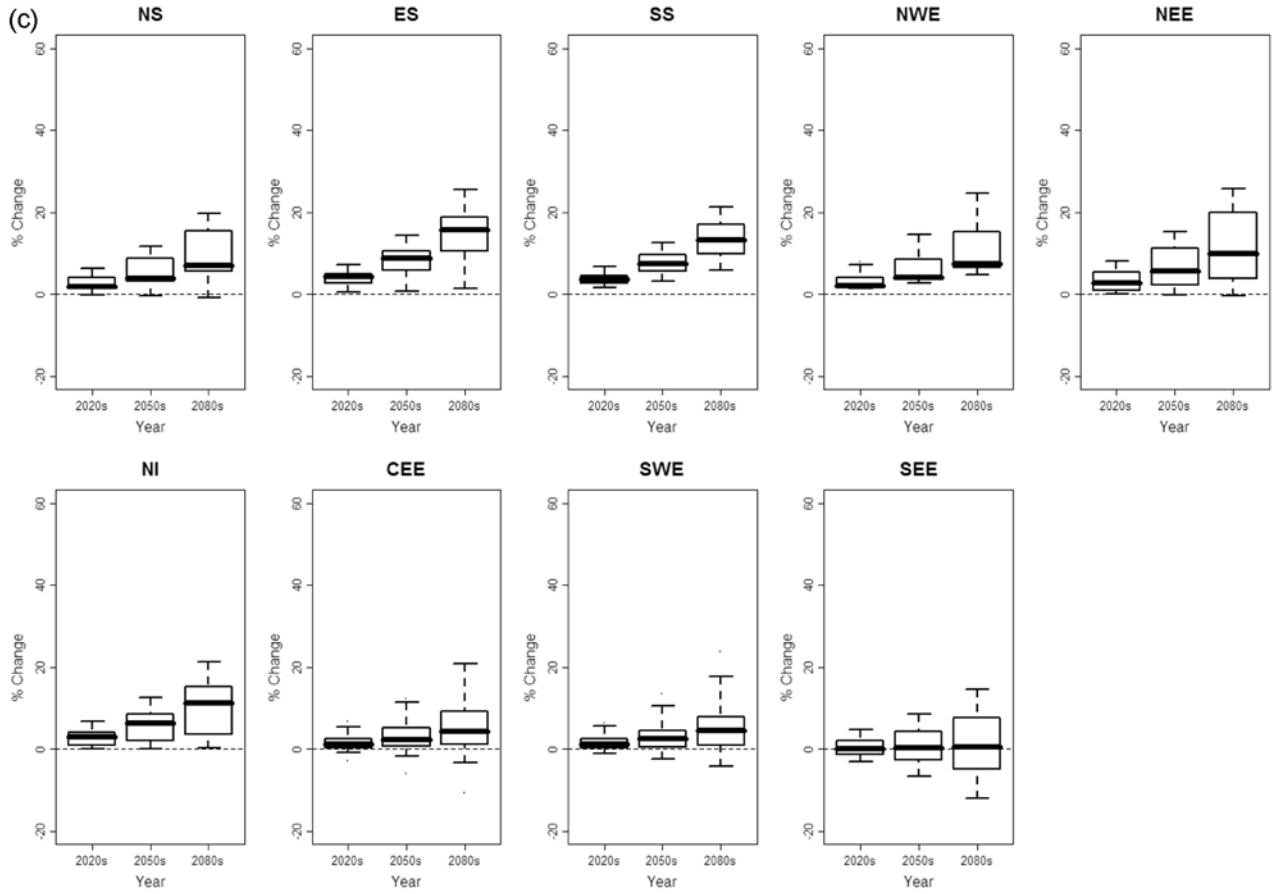

Figure 3. (continued)

standard is more likely than not, for any season and detection index. The allowances are deemed to be insufficient if the year of exceedance falls *before* the last year in the look-up table given in PPS25 (e.g., before 2025, 2055 and 2085 in the cases of the 5%, 10% and 20% allowances respectively). Although individual RCMs project exceedances earlier than this—as early as 2040 for exceedance of the 20% allowance—failure of the allowance is taken to be when more than 50% of the ensemble members show this level of exceedance.

[35] Figure 7 suggests that the national allowances may not be sufficiently robust for some regions, particularly for the earlier periods 1990–2025 and 2025–2055. The minimum year of likely exceedance of the 5% allowance is pre-2025 for ES and NEE; in other regions this allowance is typically exceeded between 2025 and 2040. Likewise, the minimum year of likely exceedance of the 10% allowance is pre-2055 for ES, NEE and also NI; in other regions this allowance is exceeded between 2055 and 2070. For the 20% allowance the minimum year of likely exceedance is 2072 for ES and 2082 for NEE, so the allowance is not sufficiently precautionary in these two regions. For other regions the allowance is exceeded in the 2090s or, in the case of SEE, not until after 2100.

5. Discussion

[36] Historic changes in UK flood risk have been reviewed elsewhere [see *Wilby et al.*, 2008]. Several studies report increasing winter precipitation, larger multiday rainfall totals, and higher contributions from intense daily events since the 1960s. Others suggest strong regional gradients with larger winter increases in the north and west of the United Kingdom, and at higher elevation sites. These patterns translate into increased winter mean runoff, especially in the upland areas of western England and Wales. One explanation is that the changes were forced by a strongly positive phase of the North Atlantic Oscillation (NAO) between the 1960s and 1990s. This displaced storm tracks northward and strengthened westerly moisture advection from the Atlantic over northwest Europe [*Haylock and Goodess*, 2004]. Whether or not recent variability in the NAO is itself a manifestation of anthropogenic forcing remains an open question [*Hegerl et al.*, 2007]. However, extensive flooding in England during summer 2007 prompted increases to budgets for flood risk management. So the question now arises as to *when* and *where* to prioritize future investment in flood defense assets?

[37] Although attribution of changes in precipitation or flood risk is not yet possible at regional scales, techniques are being developed for detection of trends in these indices at river basin scales, and for estimating the time taken for specified anthropogenic climate change signals to emerge from climate variability. This paper described a method for estimating detection times for changes in seasonal precipitation extremes projected by the European Union PRUDENCE RCM ensemble. We showed that for selected UK regions and extreme precipitation indices, climate

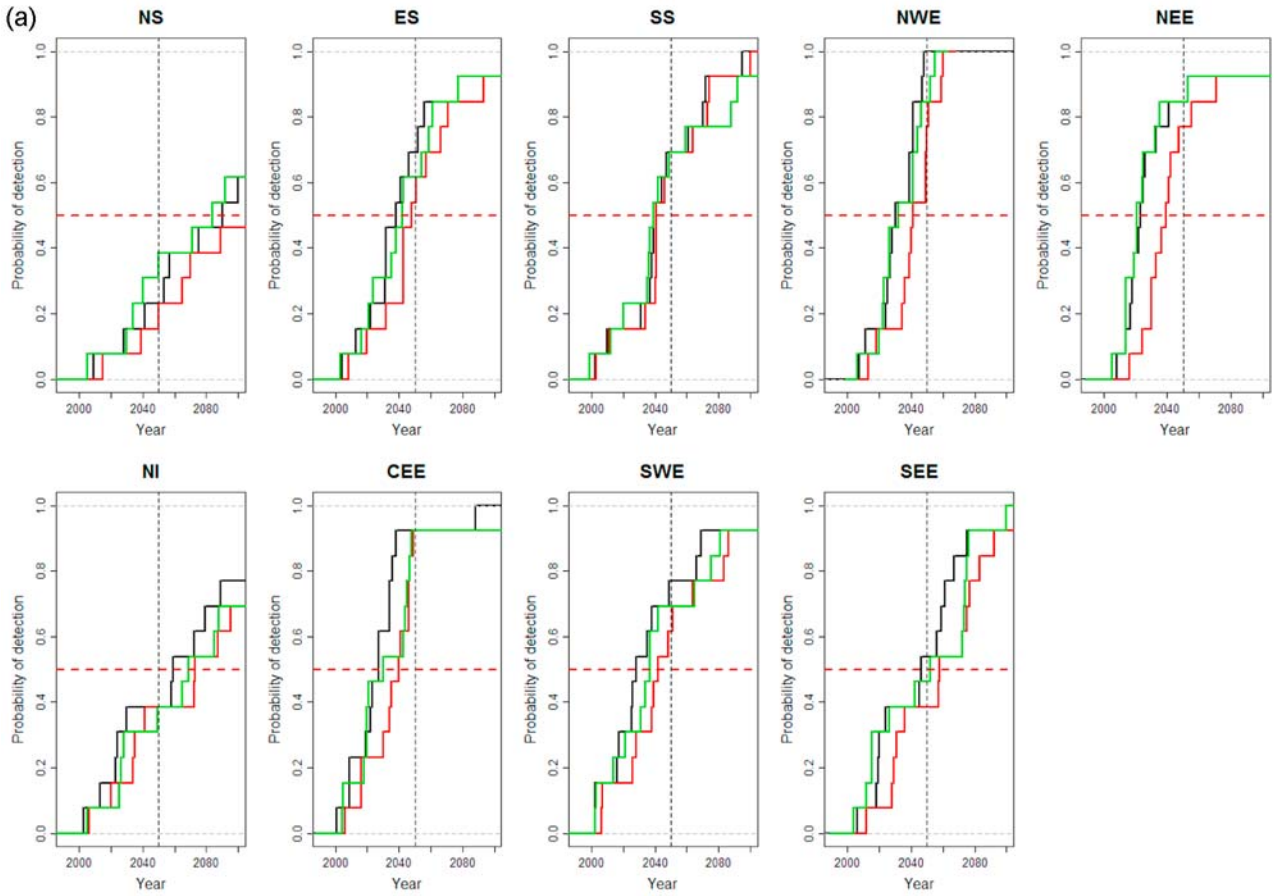

Figure 4. Detection year for significant change (α = 0.05 level) in the estimated (a) 1d10y total (top) and (b) 10d10y total (bottom) winter precipitation by region. Data used to estimate natural variability: observed 1958–2002 (black lines), RCM 1961–1990 (green lines), and observed 1961–1990 (red lines).

change signal(s) in the PRUDENCE projections could be detectable as early as the 2020s.

[38] Previous studies suggest that coherent spatial patterns are rarely found for extreme precipitation in RCM ensembles due to the local scale of such events [*Tebaldi et al.*, 2006; *Frich et al.*, 2002]. This view is supported by our findings for precipitation changes in summer which, for 1d totals, are seldom detectable before the 2050s, in any region. By implication, consistent information about changes in the type of flash flooding witnessed in summer 2007, will not emerge for many decades unless marked improvements can be made to the modeling of such convective rainfall events by, for example, improved RCM resolution or improved parameterization of convective processes. For the foreseeable future, flood managers will have to make adaptation decisions about these types of extreme event in advance of formally detected changes in flood risk. However, the situation for long duration, autumn and winter rainfall extremes, is much more promising. Changes in the 10d10y totals may well be detectable in most regions before the 2040s and even within the next decade or so in some "sentinel" regions such as SW England (Figure 8). This suggests that different precautionary allowances should be used for subdaily, daily and multiday rainfall events.

[39] We note that for detection times before the 2030s uncertainties due to the emissions scenario can be discounted, and the signal can be interpreted due to changes already locked into the climate system by past emissions. Unfortunately, the uncertainty due to the mix of models used in the PRUDENCE ensemble cannot be so readily dismissed. Given that the majority of RCM experiments were forced by HadCM3/HadAM3H, climate model uncertainty is underplayed, and so our probability distributions of detection time are almost certainly too narrow. This potentially translates into earlier detection times (because of greater model consensus) than might otherwise emerge from a much larger ensemble of host GCMs, although the two RCMs forced by ECHAM4 included within the PRUDENCE ensemble project much greater increases in extreme rainfall and thus earlier detection times than their HadCM3/HadAM3H forced counterparts. Furthermore, our method of regional pooling could lead to lower variance estimates for natural variability, and hence earlier detection for a given climate change signal (R. Chandler, personal communication, 2008) although this is probably of second- or third-order magnitude compared to other uncertainties. Both aspects merit further investigation. A natural extension to the work would be to apply the same detection method to the EU ENSEMBLES results which have been downscaled

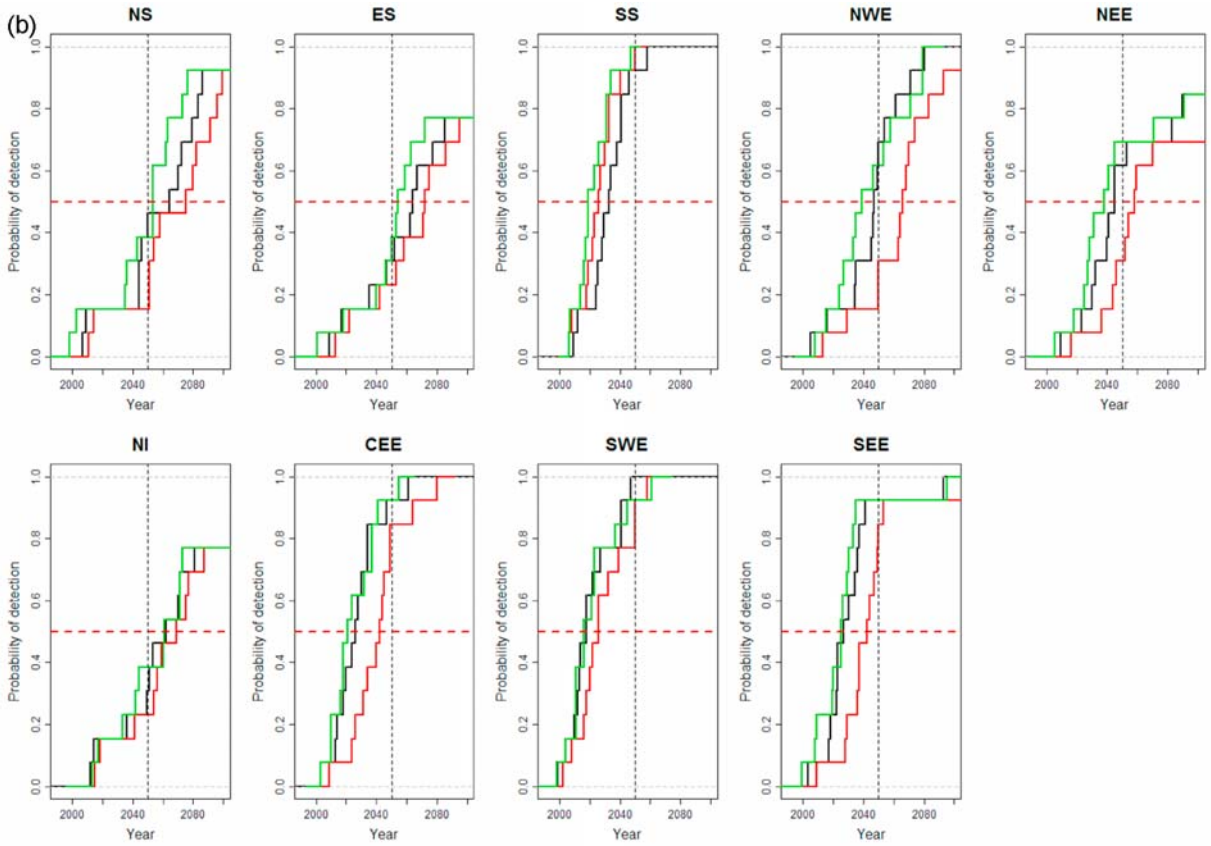

Figure 4. (continued)

Table 2. Years in Which the Probability of Detection Is >0.5 for Winter 1 and 10 Day Precipitation Totals, 10 and 50 Year Return Levels, and Three Different Variance Estimates for All Regions[a]

			Region[b]									
	Return Level	Variance Estimate	NS	ES	SS	NWE	NEE	NI	CEE	SWE	SEE	Mean D_x
Winter 1 day precipitation total	10 year	Observed (1958–2002)	2090	2038	2039	2030	2023	2059	2027	2028	2046	2042
		Observed (1961–1990)	ND	2048	2041	2041	2039	2073	2040	2042	2058	2055
		RCM Estimated	2084	2042	2039	2032	2021	2069	2030	2037	2052	2045
	50 year	Observed (1958–2002)	ND	2069	2059	2049	2046	2066	2030	2066	2061	2062
		Observed (1961–1990)	ND	2084	2058	2062	2067	2082	2044	2087	2081	2075
		RCM Estimated	ND	2075	2063	2057	2042	2091	2054	2069	2066	2070
Winter 10 day precipitation total	10 year	Observed (1958–2002)	2064	2064	2033	2047	2045	2062	2026	2018	2027	2043
		Observed (1961–1990)	2075	2072	2026	2066	2058	2069	2042	2026	2042	2053
		RCM Estimated	2053	2054	2019	2039	2038	2061	2021	2016	2025	2036
	50 year	Observed (1958–2002)	2086	2096	2052	2061	2076	2088	2048	2025	2050	2065
		Observed (1961–1990)	2100	ND	2036	2098	ND	2089	2071	2040	2076	2081
		RCM Estimated	2075	2079	2028	2058	2076	2078	2045	2030	2048	2057
Earliest detection time[c]			2030 Aut	2032 Aut	2019 Win	2030 Win	2021 Win	2033 Spr	2021 Win	2016 Win	2025 Win	2036 Win

[a]ND indicates that the probability of detection is <0.5 by 2100 (i.e., "not detected"). The earliest detection time and the season (Win, winter; Spr, spring; and Aut, autumn) in which change is detected is also summarized. Note that for calculation of mean D_x the conservative assumption was made that ND = 2110.

[b]See Figure 1 caption for region definitions.

[c]For all seasons, precipitation totals and variance estimates.

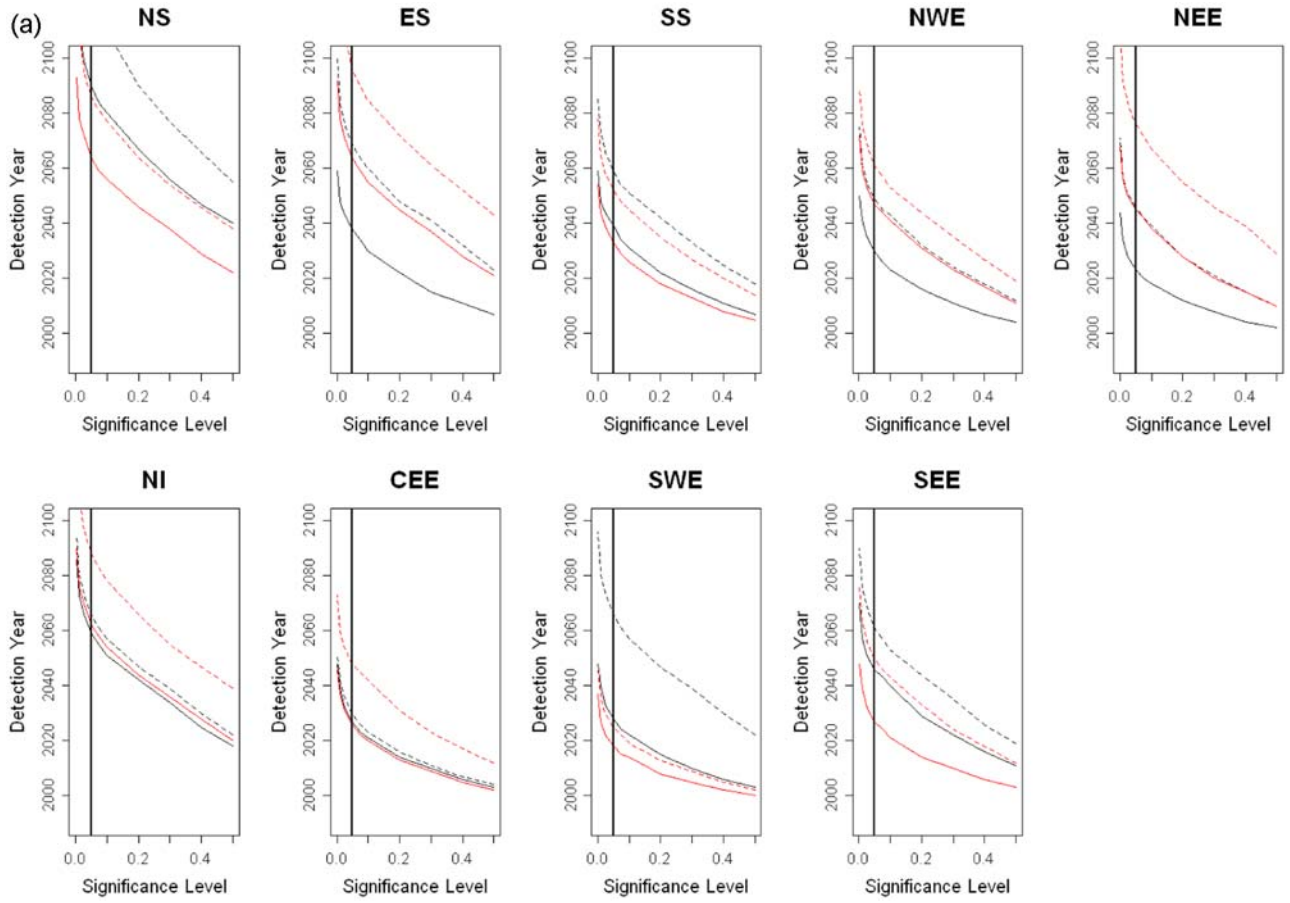

Figure 5. The sensitivity of detection year, D_x, to the α significance level used in testing "detectability" for (a) winter extremes and (b) spring extremes: 1d10y (black solid line), 1d50y (black dashed line), 10d10y (red solid line), and 10d50y totals (red dashed line).

from a much larger selection of GCMs [*Hewitt and Griggs*, 2004].

[40] In addition it should be noted that for detection times beyond the 2030s, uncertainties due to the emissions scenario are important. Here we use only the SRES A2 emissions scenario which is "medium-high." However, there is evidence to suggest that all SRES emissions scenarios underestimate the amount of warming that is already being observed, both in western Europe [*Oldenborgh et al.*, 2008] and globally [*Rahmstorf et al.*, 2007]. This is doubly important when we consider that climate models and satellite observations both indicate that the total amount of water in the atmosphere will increase at a rate of 7% per °C of surface warming (the so-called Clausius-Clapeyron constant). However, although global climate models suggest that precipitation will increase at only 1 to 3% per °C of surface warming, satellite and gauge observations suggest that precipitation has increased at around the Clausius-Clapeyron rate over the last 20 years [*Wentz et al.*, 2007]. Climate models also suggest that extreme precipitation events will become more common in a warmer world. Satellite observations [*Allan and Soden*, 2008] and gauge observations [*Lenderink and van Meijgaard*, 2008] indicate that the observed increase in daily extreme precipitation is larger than that simulated by climate models, implying that projections of future changes in precipitation extremes in response to global warming may be underestimated. Furthermore, observed hourly extremes have increased by 14%, which is a rate twice that of Clausius-Clapeyron [*Lenderink and van Meijgaard*, 2008]. Regional climate models are unable to adequately reproduce this rate of change for temperatures above 20°C. This is particularly relevant to summer months for which RCMs cannot adequately reproduce daily extreme precipitation events [*Fowler and Ekström*, 2009]. For these reasons it is likely that absolute changes to extreme precipitation by the 2080s may well be underestimated by this study. However, over the next decade or so, an anticipated cool downturn across northwest Europe [*Keenlyside et al.*, 2008], could favor a temporary reduction to precipitation extremes.

[41] By identifying potential "hotspots" of emerging flood risk, a more targeted approach to monitoring and investment planning might be feasible. A further priority is to broaden the analysis to include a larger suite of extreme indicators that can be linked to different types of flood generation mechanism [e.g., see *Bárdossy and Filiz*, 2005]. For example, long-term changes in extreme rainfall combined with snowmelt might not exhibit the smooth transitions inferred from the rainfall-only indices applied herein. Rising temperatures could bring forward the spring melt, and increase

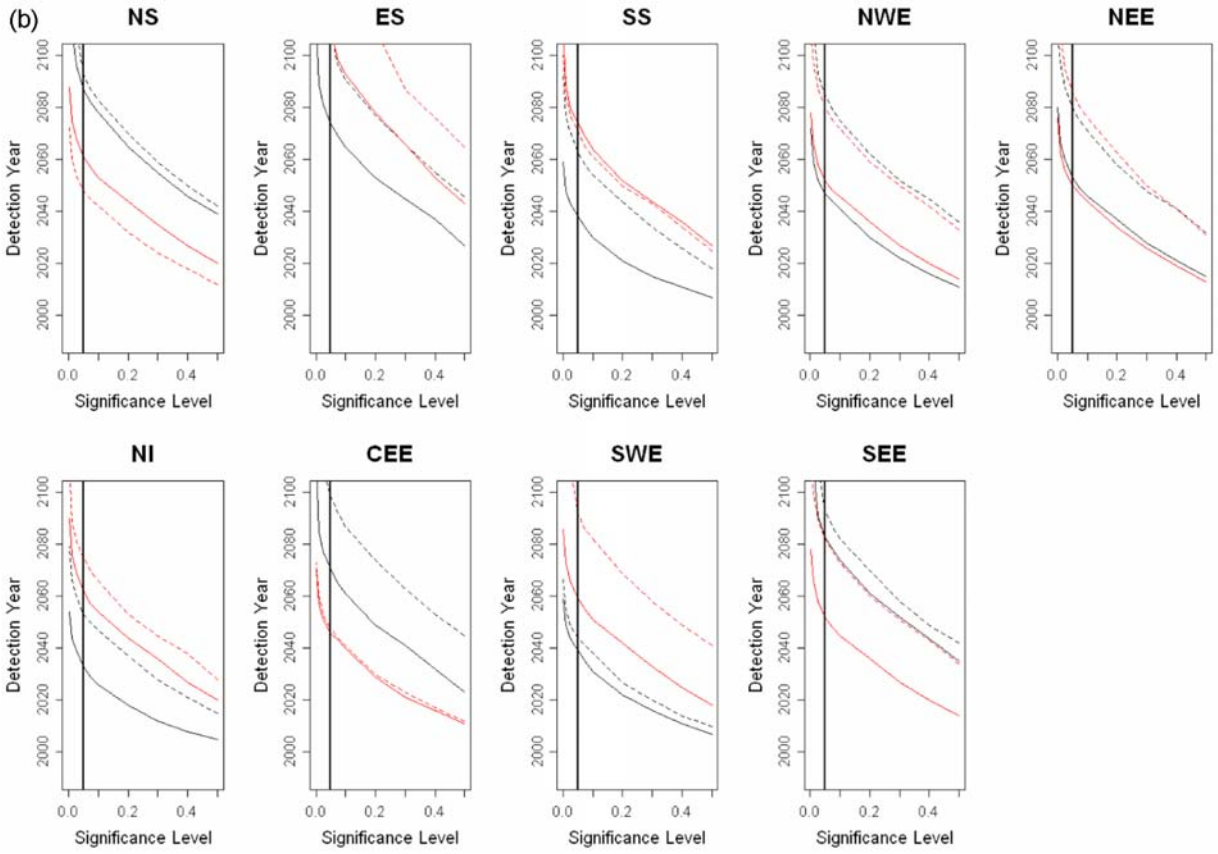

Figure 5. (continued)

the fraction of liquid precipitation in upland areas, thereby increasing flood peaks in the short term as has already been reported in North America [*Zhang et al.*, 2001]. Over the medium to longer term, the net effect of more intense winter rainfall combined with less water storage in the snowpack could be *lower* levels of flood risk [e.g., see *Dankers and Feyen*, 2008]. All of these concerns underline the importance of long-term monitoring and reporting of environmental changes at sentinel locations. Furthermore, precautionary allowances for climate change should be routinely examined in the light of emerging trends and the latest climate model projections.

6. Concluding Remarks

[42] This paper described a methodology for estimating detection times for future changes in seasonal precipitation extremes. The approach was illustrated using the precipitation projections of the European Union PRUDENCE ensemble for homogeneous rainfall regions in the United Kingdom. By optimizing the choice of detection index, season and region it was shown that the earliest detections could occur within a decade. The same ensemble warns that the climate change allowances currently used in flood defense design may not be sufficiently precautionary within their intended time horizons (for NE England and East Scotland). Therefore, one practical recommendation from this research is that a suite of national detection indices is established and then used to monitor and report changes in pluvial flood risk. This would provide evidence for testing the provenance of climate model projections, and a means for targeting future investment in adaptation responses.

Appendix A

[43] Regional frequency analysis (RFA) usually follows a two part *index-flood* procedure [*Hosking and Wallis*, 1997]. If data are available at N grid cells, with grid cell i having sample size n_i and observed data, X_{ij}, $j = 1,\ldots,n_i$, then $X_i(F)$, $0 < F < 1$, forms the frequency distribution's quantile function at grid cell i. The grid cells are assumed to form a homogeneous region, with identical frequency distributions at the N grid cells apart from the site specific scaling factor, the *index-flood* [*Hosking and Wallis*, 1997]. For the United Kingdom, nine climatological regions delineated by *Wigley et al.* [1984] (Figure 1) have been checked for homogeneity of extreme precipitation by *Fowler and Kilsby* [2003a].

[44] The index-flood procedure may then be defined as [*Hosking and Wallis*, 1997]

$$X_i(F) = Rmed_i x(F),\ i = 1,\ldots,N, \qquad \text{(A1)}$$

where $Rmed_i$ is the index-flood (here it is the median of the seasonal maxima frequency distribution for an individual grid cell, i), and $x(F)$ is the regional growth curve, a quantile

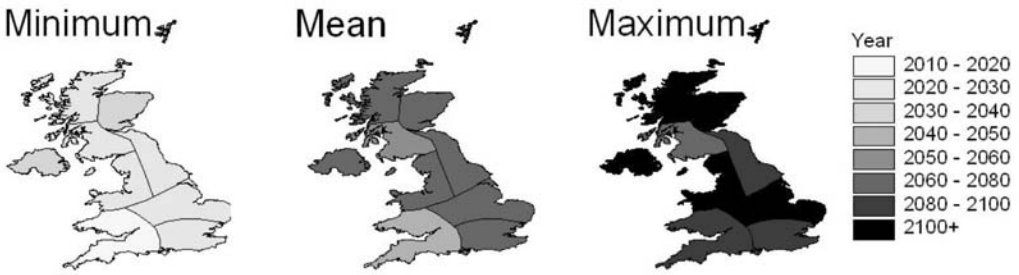

Figure 6. The minimum, mean, and maximum year in which the probability of detection is more likely than not for any season, rainfall aggregation or return level, given $\alpha = 0.05$ and natural variability based on observations (1958–2002). Note that for calculation of mean and maximum D_x the conservative assumption was made that ND = 2110.

function assumed identical at every grid cell within that region.

[45] For each RCM time-slice (the control period, 1961–1990, and future period, 2071–2100) and for observations, the same RFA procedure is then followed for each season and precipitation total in turn.

[46] 1. Seasonal maximum (SM) series of 1, 5 and 10 day (henceforth 1d, 5d and 10d) precipitation totals are extracted for each grid cell.

[47] 2. The SM series for each grid cell, i, is standardized by its median ($Rmed_i$, which is equivalent to the 2 year return value [after *Fowler et al.*, 2005]) to remove grid cell–specific factors from the regional analysis.

[48] 3. The standardized SM data for the N grid cells within an individual region for each of the nine UK rainfall regions is "pooled."

[49] 4. The *regional growth curve,* $x(F)$, $0 < F < 1$ is then derived, using a pooled analysis of the dimensionless rescaled data, $x_{ij} = X_{ij}/Rmed_i$, $j = 1,\ldots,n_i$, $i = 1,\ldots,N$. A Generalized Extreme Value (GEV) distribution is fitted to the standardized SM data set for each regional "pool," x_{ij}, using Maximum Likelihood Estimation (MLE). This is used to estimate return values of precipitation intensities with average recurrence of 10 and 50 years (henceforth 10y and 50y).

[50] 5. Return value estimates at grid cell i are obtained by combining the estimates of $Rmed_i$ and $x(F)$ as equation (A1). The average regional growth curve can be obtained by combining the estimates of $x(F)$ and the regional average Rmed: $\sum_1^N Rmed_i \Big/ N$.

[51] 6. The associated error and 95% confidence intervals for the return value estimates is calculated using the delta method [*Oehlert*, 1992] for three estimates of variance to test sensitivity to (1) RCM-estimated internal variability from pooled sample variance; (2) observed variance, 1961–

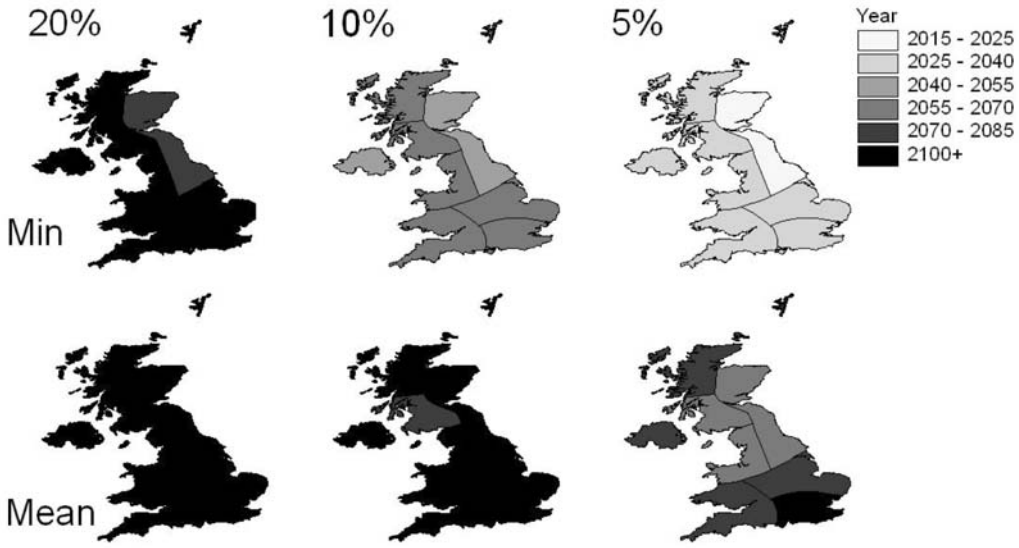

Figure 7. (top) The minimum year and (bottom) the mean year in which probability of exceedance of the 5%, 10%, and 20% climate change allowances from PPS25 used for flood risk management is >0.5 for all seasons, rainfall aggregations, and return levels. Change is calculated at the $\alpha = 0.05$ level using the observed (1958–2002) estimate of natural variability.

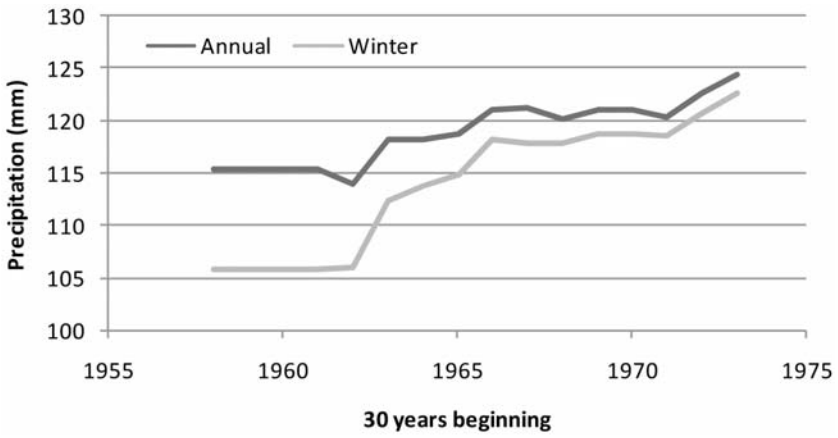

Figure 8. Changes in the annual and winter 10d10yr precipitation totals in SW England. Values were estimated by fitting a GEV distribution to observed precipitation data falling within 30 year moving windows that are advanced 1 year at a time from 1958 onward. For example, the extreme value plotted for 1958 was estimated from annual maximum series for the period 1958–1987, that for 1959 from annual maxima from 1959 to 1988, and so on. The indices suggest ~20% increase in the precipitation accumulated during winter episodes typically marked by successive days of cyclonic systems (as during the widespread United Kingdom flooding of autumn/winter 2000/2001).

1990; (3) observed variance, 1958–2002 (full length of record). Note that the variance based on the longer observation set gives a more conservative estimate of confidence intervals compared to the variance derived from the RCM pooled sample.

[52] **Acknowledgments.** RCM data were obtained from the PRUDENCE project archive (http://prudence.dmi.dk/) which was supported by EU contract EVk2-CT2001-00132. Development of the UKMO 5 km data sets was supported by the Department of Environment, Food and Rural Affairs. These data form part of the UKCIP02 national climate scenarios prepared on behalf of UK Climate Impacts Programme by the Tyndall and Hadley Centres. We thank Andy Smith, Ph.D. student at Newcastle, for producing the aggregated observed precipitation data and Stephen Blenkinsop for regridding the RCM data to the common CRU grid for the European Union FP6 Integrated Project AquaTerra (project 505428). Data on global temperature changes were obtained from the IPCC Data Distribution Centre (http://www.ipcc-data.org/). This study was supported by a NERC Postdoctoral Fellowship award to Hayley Fowler (2006–2009) NE/D009588/1 and by Environment Agency contract 21717.

References

Alexander, L. V., et al. (2006), Global observed changes in daily climate extremes of temperature and precipitation, *J. Geophys. Res.*, *111*, D05109, doi:10.1029/2005JD006290.

Allan, R. P., and B. J. Soden (2008), Atmospheric warming and the amplification of precipitation extremes, *Science*, *321*, 1481–1484, doi:10.1126/science.1160787.

Arribas, A., C. Gallardo, M. A. Gaertner, and M. Castro (2003), Sensitivity of Iberian Peninsula climate to land degradation, *Clim. Dyn.*, *20*, 477–489.

Bárdossy, A., and F. Filiz (2005), Identification of flood producing atmospheric circulation patterns, *J. Hydrol.*, *313*, 48–57, doi:10.1016/j.jhydrol.2005.02.006.

Burke, E. J., S. J. Brown, and N. Christidis (2006), Modelling the recent evolution of global drought and projections for the 21st century with the Hadley Centre climate model, *J. Hydrometeorol.*, *7*, 1113–1125, doi:10.1175/JHM544.1.

Castro, M., C. Fernández, and M. A. Gaertner (1993), Description of a meso-scale atmospheric numerical model, in *Mathematics, Climate and Environment*, edited by J. I. Díaz and J. L. Lions, pp. 230–253, Masson, Paris.

Chiew, F. H. S., and T. A. McMahon (1993), Detection of trend or change in annual flow of Australian rivers, *Int. J. Climatol.*, *13*, 643–653, doi:10.1002/joc.3370130605.

Christensen, J. H., O. B. Christensen, P. Lopez, E. van Meijgaard, and M. Botzet (1996), The HIRHAM4 regional atmospheric climate model, *Tech. Rep. 96–4*, Dan. Meteorol. Inst., Copenhagen.

Christensen, J. H., O. B. Christensen, and J. P. Schultz (2001), High resolution physiographic data set for HIRHAM4: An application to a 50 km horizontal resolution domain covering Europe, *Tech. Rep. 01–15*, Dan. Meteorol. Inst., Copenhagen.

Christensen, J. H., T. R. Carter, M. Rummukainen, and G. Amanatidis (2007), Evaluating the performance and utility of regional climate models: The PRUDENCE project, *Clim. Change*, *81*, 1–6, doi:10.1007/s10584-006-9211-6.

Christensen, O. B., J. H. Christensen, B. Machenhauer, and M. Botzet (1998), Very high-resolution regional climate simulations over Scandinavia: Present climate, *J. Clim.*, *11*, 3204–3229, doi:10.1175/1520-0442(1998)011<3204:VHRRCS>2.0.CO;2.

Coulthard, T., L. Frostick, H. Hardcastle, K. Jones, D. Rogers, and M. Scott (2007), *The June 2007 floods in Hull*, 68 pp., final report, Hull City Council, Hull, UK.

Dankers, R., and L. Feyen (2008), Climate change impact on flood hazard in Europe: An assessment based on high-resolution climate simulations, *J. Geophys. Res.*, *113*, D19105, doi:10.1029/2007JD009719.

Department of Communities and Local Government (DCLG) (2006), Planning policy statement 25: Development and flood risk–Annex B: Climate change, report, 50 pp., Stationary Off., London.

Department of Environment, Food and Rural Affairs (DEFRA) (2006), FCDPAG3 economic appraisal supplementary note to operating authorities–Climate change impacts, report, London. (Available at http://www.sdcg.org.uk/Climate-change-update.pdf)

Déqué, M., P. Marquet, and R. G. Jones (1998), Simulation of climate change over Europe using a global variable resolution general circulation model, *Clim. Dyn.*, *14*, 173–189, doi:10.1007/s003820050216.

Döscher, R., U. Willén, C. Jones, A. Rutgersson, H. E. M. Meier, M. Hansson, and L. P. Graham (2002), The development of the coupled regional ocean-atmosphere model RCAO, *Boreal Environ. Res.*, *7*, 183–192.

Ekström, M., H. J. Fowler, C. G. Kilsby, and P. D. Jones (2005), New estimates of future changes in extreme rainfall across the UK using regional climate model integrations. 2. Future estimates and use in impact studies, *J. Hydrol.*, *300*(1–4), 234–251.

Environment Agency (EA) (2007), *Review of Summer 2007 Floods*, 58 pp., Bristol, UK.

European Environment Agency (2005), Vulnerability and adaptation to climate change: Scoping report, *EEA Tech. Rep. 7*, Copenhagen.

Fowler, H. J., and M. Ekström (2009), Multi-model ensemble estimates of climate change impacts on UK seasonal rainfall extremes, *Int. J. Climatol.*, *29*, 385–416, doi:10.1002/joc.1827.

Fowler, H. J., and C. G. Kilsby (2003a), A regional frequency analysis of United Kingdom extreme rainfall from 1961 to 2000, *Int. J. Climatol.*, *23*, 1313–1334, doi:10.1002/joc.943.

Fowler, H. J., and C. G. Kilsby (2003b), Implications of changes in seasonal and annual extreme rainfall, *Geophys. Res. Lett.*, *30*(13), 1720, doi:10.1029/2003GL017327.

Fowler, H. J., M. Ekström, C. G. Kilsby, and P. D. Jones (2005), New estimates of future changes in extreme rainfall across the UK using regional climate model integrations. 1. Assessment of control climate, *J. Hydrol.*, *300*, 212–233, doi:10.1016/j.jhydrol.2004.06.017.

Fowler, H. J., M. Ekström, S. Blenkinsop, and A. P. Smith (2007), Estimating change in extreme European precipitation using a multimodel ensemble, *J. Geophys. Res.*, *112*, D18104, doi:10.1029/2007JD008619.

Frei, C., and C. Schär (2001), Detection probability of trends in rare events: Theory and application to heavy precipitation in the Alpine region, *J. Clim.*, *14*, 1568–1584, doi:10.1175/1520-0442(2001)014<1568:DPOTIR>2.0.CO;2.

Frich, P., L. V. Alexander, P. Della-Marta, B. Gleason, M. Haylock, A. M. G. Klein Tank, and T. Peterson (2002), Observed coherent changes in climatic extremes during the second half of the twentieth century, *Clim. Res.*, *19*, 193–212, doi:10.3354/cr019193.

Giorgi, F., M. R. Marinucci, and G. T. Bates (1993a), Development of a second generation regional climate model (REGCM2). Part I: Boundary layer and radiative transfer processes, *Mon. Weather Rev.*, *121*, 2794–2813, doi:10.1175/1520-0493(1993)121<2794:DOASGR>2.0.CO;2.

Giorgi, F., M. R. Marinucci, G. T. Bates, and G. DeCanio (1993b), Development of a second generation regional climate model (REGCM2). Part II: Convective processes and assimilation of lateral boundary conditions, *Mon. Weather Rev.*, *121*, 2814–2832, doi:10.1175/1520-0493(1993)121<2814:DOASGR>2.0.CO;2.

Gloucestershire County Council (GCC) (2007), *Scrutiny Inquiry into the Summer Emergency 2007*, 148 pp., Overview and Scrutiny Manage. Comm., Gloucester, UK.

Groisman, P. Y., R. W. Knight, D. R. Easterling, T. R. Karl, G. C. Hegerl, and V. N. Razuvaev (2005), Trends in intense precipitation in the climate record, *J. Clim.*, *18*, 1326–1350, doi:10.1175/JCLI3339.1.

Hagemann, S., M. Botzet, and B. Machenhauer (2001), The summer drying problem over south-eastern Europe: Sensitivity of the limited area model HIRHAM4 to improvements in physical parametrization and resolution, *Phys. Chem. Earth, Part B*, *26*, 391–396.

Hanssen-Bauer, I., E. Førland, J. E. Haugen, and O. E. Tveito (2003), Temperature and precipitation scenarios for Norway: Comparison of results from dynamical and empirical downscaling, *Clim. Res.*, *25*, 15–27, doi:10.3354/cr025015.

Haylock, M., and C. Goodess (2004), Interannual variability of European extreme winter rainfall and links with mean large-scale circulation, *Int. J. Climatol.*, *24*, 759–776, doi:10.1002/joc.1033.

Hegerl, G. C., F. W. Zwiers, P. A. Stott, and V. V. Kharin (2004), Detectability of anthropogenic changes in annual temperature and precipitation extremes, *J. Clim.*, *17*, 3683–3700, doi:10.1175/1520-0442(2004)017<3683:DOACIA>2.0.CO;2.

Hegerl, G. C., T. R. Karl, M. Allen, N. L. Bindoff, N. Gillett, D. Karoly, X. B. Zhang, and F. Zwiers (2006), Climate change detection and attribution: Beyond mean temperature signals, *J. Clim.*, *19*, 5058–5077, doi:10.1175/JCLI3900.1.

Hegerl, G. C., F. W. Zwiers, P. Braconnot, N. P. Gillet, Y. Luo, J. A. Marengo, N. Nicholls, J. E. Penner, and P. A. Stott (2007), Understanding and attributing climate change, in *Climate Change 2007: The Physical Basis. Contribution of Working Group I to the Fourth Assessment of the Intergovernmental Panel on Climate Change*, edited by S. Solomon et al., pp. 663–745, Cambridge Univ. Press, New York.

Hewitt, C. D., and D. J. Griggs (2004), Ensembles-based predictions of climate changes and their impacts, *Eos Trans. AGU*, *85*, 566, doi:10.1029/2004EO520005.

Hosking, J. R. M., and J. R. Wallis (1997), *Regional Frequency Analysis: An Approach Based on L-Moments*, 224 pp., Cambridge Univ. Press, Cambridge, UK.

Jacob, D. (2001), A note to the simulation of the annual and inter-annual variability of the water budget over the Baltic Sea drainage basin, *Meteorol. Atmos. Phys.*, *77*, 61–73, doi:10.1007/s007030170017.

Jacob, D., et al. (2007), An inter-comparison of regional climate models for Europe: Model performance in present-day climate, *Clim. Change*, *81*, 31–52, doi:10.1007/s10584-006-9213-4.

Jones, C. G., A. Ullerstig, U. Willén, and U. Hansson (2004b), The Rossby Centre regional atmospheric climate model (RCA). Part I: Model climatology and performance characteristics for present climate over Europe, *Ambio*, *33*, 199–210.

Jones, R. G., M. Noguer, D. C. Hassell, D. Hudson, S. S. Wilson, G. J. Jenkins, and J. F. B. Mitchell (2004a), Generating high resolution climate change scenarios using PRECIS, technical report, 35 pp., Met Off. Hadley Centre, Exeter, UK.

Katz, R. W. (1999), Extreme value theory for precipitation: Sensitivity analysis for climate change, *Adv. Water Resour.*, *23*, 133–139, doi:10.1016/S0309-1708(99)00017-2.

Keenlyside, N. S., M. Latif, J. Jungclaus, L. Kornblueh, and E. Roeckner (2008), Advancing decadal-scale climate prediction in the North Atlantic sector, *Nature*, *453*, 84–88, doi:10.1038/nature06921.

Kharin, V. V., and F. W. Zwiers (2000), Changes in the extremes in an ensemble of transient climate simulation with a coupled atmosphere-ocean GCM, *J. Clim.*, *13*, 3760–3788, doi:10.1175/1520-0442(2000)013<3760:CITEIA>2.0.CO;2.

Kiktev, D., D. Sexton, L. Alexander, and C. Folland (2003), Comparison of modelled and observed trends in indices of daily climate extremes, *J. Clim.*, *16*, 3560–3571, doi:10.1175/1520-0442(2003)016<3560:COMAOT>2.0.CO;2.

Kundzewicz, Z. W., and A. J. Robson (2004), Change detection in hydrological records—A review of the methodology, *Hydrol. Sci. J.*, *49*, 7–19, doi:10.1623/hysj.49.1.7.53993.

Lambert, F. H., P. A. Stott, M. R. Allen, and M. A. Palmer (2004), Detection and attribution of changes in 20th century land precipitation, *Geophys. Res. Lett.*, *31*, L10203, doi:10.1029/2004GL019545.

Legates, D. R., H. F. Lins, and G. J. McCabe (2005), Comments on "Evidence for global runoff increase related to climate warming" by Labat et al, *Adv. Water Resour.*, *28*, 1310–1315, doi:10.1016/j.advwatres.2005.04.006.

Lenderink, G., and E. van Meijgaard (2008), Increase in hourly precipitation extremes beyond expectations from temperature changes, *Nat. Geosci.*, *1*, 511–514, doi:10.1038/ngeo262.

Lenderink, G., B. van den Hurk, E. van Meijgaard, A. P. van Ulden, and J. Cuijpers (2003), Simulation of present-day climate in RACMO2: First results and model developments, *Tech. Rep. 252*, 24 pp., K. Ned. Meteorol. Inst., De Bilt, Neth.

Lüthi, D., A. Cress, H. C. Davies, C. Frei, and C. Schär (1996), Interannual Variability and Regional Climate Simulations, *Theor. Appl. Climatol.*, *53*, 185–209, doi:10.1007/BF00871736.

Manning, L., J. W. Hall, H. J. Fowler, C. G. Kilsby, and C. Tebaldi (2009), Using probabilistic climate change information from a multimodel ensemble for water resources assessment, *Water Resour. Res.*, *45*, W11411, doi:10.1029/2007WR006674.

Marsh, T., G. Cole, and R. L. Wilby (2007), Major droughts in England and Wales, 1800–2006, *Weather*, *62*, 87–93, doi:10.1002/wea.67.

Meier, H. E. M., R. Döscher, and T. Faxén (2003), A multiprocessor coupled ice-ocean model for the Baltic Sea: Application to the salt inflow, *J. Geophys. Res.*, *108*(C8), 3273, doi:10.1029/2000JC000521.

Mitchell, T. D. (2003), Pattern scaling: An examination of the accuracy of the technique for describing future climates, *Clim. Change*, *60*, 217–242, doi:10.1023/A:1026035305597.

Moberg, A., and P. D. Jones (2004), Regional climate models simulations of daily maximum and minimum near-surface temperatures across Europe compared with observed station data for 1961–1990, *Clim. Dyn.*, *23*, 695–715, doi:10.1007/s00382-004-0464-3.

Nakićenović, N., et al. (2000), *Emissions Scenarios. A Special Report of Working Group III of the Intergovernmental Panel on Climate Change*, 559 pp., Cambridge Univ. Press, Cambridge, UK.

Oehlert, G. W. (1992), A note on the delta method, *Am. Stat.*, *46*, 27–29, doi:10.2307/2684406.

Oldenborgh, G. J., S. S. van Drijfhout, A. van Ulden, R. Haarsma, A. Sterl, C. Severijns, W. Hazeleger, and H. Dijkstra (2008), Western Europe is warming much faster than expected, *Clim. Past Discuss.*, *4*, 897–928.

Pal, J. S., E. E. Small, and E. A. B. Eltahir (2000), Simulation of regional-scale water and energy budgets: Representation of subgrid cloud and precipitation processes within RegCM, *J. Geophys. Res.*, *105*, 29,579–29,594, doi:10.1029/2000JD900415.

Pall, P., M. R. Allen, and D. A. Stone (2007), Testing the Clausius-Clapeyron constraint on changes in extreme precipitation under CO2 warming, *Clim. Dyn.*, *28*, 351–363, doi:10.1007/s00382-006-0180-2.

Perry, M., and D. Hollis (2005a), The development of a new set of long-term climate averages for the UK, *Int. J. Climatol.*, *25*, 1023–1039, doi:10.1002/joc.1160.

Perry, M., and D. Hollis (2005b), The generation of monthly gridded datasets for a range of climatic variables over the UK, *Int. J. Climatol.*, *25*, 1041–1054, doi:10.1002/joc.1161.

Radziejewski, M., and Z. W. Kundzewicz (2004), Detectability of changes in hydrological records, *Hydrol. Sci. J.*, *49*, 39–51, doi:10.1623/hysj.49.1.39.54002.

Rahmstorf, S., A. Cazenave, J. A. Church, J. E. Hansen, R. F. Keeling, D. E. Parker, and R. C. J. Somerville (2007), Recent Climate Observations Compared to Projections, *Science*, *316*, 709, doi:10.1126/science.1136843.

Räisänen, J., U. Hansson, A. Ullerstig, R. Döscher, L. P. Graham, C. Jones, M. Meier, P. Samuelsson, and U. Willén (2004), European climate in the late 21st century: Regional simulations with two driving global models and two forcing scenarios, *Clim. Dyn.*, *22*, 13–31, doi:10.1007/s00382-003-0365-x.

Roeckner, E., K. Arpe, L. Bengtsson, M. Christoph, M. Claussen, L. Dümenil, M. Esch, M. Giorgetta, U. Schlese, and U. Schulzweida (1996), The atmospheric general circulation model ECHAM4: Model description and simulation of present-day climate, *Rep. 218*, 90 pp., Max Planck Inst. für Meteorol., Hamburg, Ger.

Santer, B. D., et al. (2007), Identification of human-induced changes in atmospheric moisture content, *Proc. Natl. Acad. Sci. U. S. A.*, *104*, 15,248–15,253, doi:10.1073/pnas.0702872104.

Steppeler, J., G. Doms, U. Schättler, H. W. Bitzer, A. Gassmann, U. Damrath, and G. Gregoric (2003), Meso-gamma scale forecasts using the nonhydrostatic model LM, *Meteorol. Atmos. Phys.*, *82*, 75–96, doi:10.1007/s00703-001-0592-9.

Svensson, C., Z. W. Kundzewicz, and T. Maurer (2005), Trend detection in river flow series: 2. Flood and low-flow index series, *Hydrol. Sci. J.*, *50*, 811–824, doi:10.1623/hysj.2005.50.5.811.

Tebaldi, C., K. Hayhoe, J. M. Arblaster, and G. A. Meehl (2006), Going to extremes: An intercomparison of model-simulated historical and future changes in extreme events, *Clim. Change*, *79*, 185–211, doi:10.1007/s10584-006-9051-4.

Tett, S. F. B., R. Betts, T. J. Crowley, J. Gregory, T. C. Johns, A. Jones, T. J. Osborn, E. Ostrom, D. L. Roberts, and M. J. Woodgate (2007), The impact of natural and anthropogenic forcings on climate and hydrology since 1550, *Clim. Dyn.*, *28*, 3–34, doi:10.1007/s00382-006-0165-1.

Tiedtke, M. (1989), A comprehensive mass flux scheme for cumulus parameterization in large-scale models, *Mon. Weather Rev.*, *117*, 1779–1800, doi:10.1175/1520-0493(1989)117<1779:ACMFSF>2.0.CO;2.

Tiedtke, M. (1993), Representation of clouds in large-scale models, *Mon. Weather Rev.*, *121*, 3040–3061, doi:10.1175/1520-0493(1993)121<3040:ROCILS>2.0.CO;2.

Timbal, B., J. M. Arblaster, and S. Power (2006), Attribution of late 20th century rainfall decline in South–West Australia, *J. Clim.*, *19*, 2046–2062, doi:10.1175/JCLI3817.1.

Trenberth, K. E., A. Dai, R. M. Rasmussen, and D. B. Parsons (2003), The changing character of precipitation, *Bull. Am. Meteorol. Soc.*, *84*, 1205–1217, doi:10.1175/BAMS-84-9-1205.

Vidale, P. L., D. Lüthi, C. Frei, S. Seneviratne, and C. Schär (2003), Predictability and uncertainty in a regional climate model, *J. Geophys. Res.*, *108*(D18), 4586, doi:10.1029/2002JD002810.

Wehner, M. F. (2004), Predicted 21st century changes in seasonal extreme precipitation events in the Parallel Climate Model, *J. Clim.*, *17*, 4281–4290, doi:10.1175/JCLI3197.1.

Wentz, F. J., L. Ricciardulli, K. Hilburn, and C. Mears (2007), How much more rain will global warming bring?, *Science*, *317*, 233–235, doi:10.1126/science.1140746.

Wigley, T. M. L., J. M. Lough, and P. D. Jones (1984), Spatial patterns of precipitation in England and Wales and a revised, homogeneous England and Wales precipitation series, *J. Climatol.*, *4*, 1–25, doi:10.1002/joc.3370040102.

Wilby, R. L. (2006), When and where might climate change be detectable in UK river flows?, *Geophys. Res. Lett.*, *33*, L19407, doi:10.1029/2006GL027552.

Wilby, R. L., K. J. Beven, and N. S. Reynard (2008), Climate change and fluvial flood risk in the UK: More of the same?, *Hydrol. Process.*, *22*, 2511–2523, doi:10.1002/hyp.6847.

Wilby, R. L., H. J. Fowler, and B. Donovan (2010), Uncertainty in the detection times for changing precipitation extremes in the UK, in *Applied Uncertainty Analysis for Flood Risk Management*, edited by K. J. Beven and J. Hall, World Sci., London, in press.

Willett, K. M., N. P. Gillett, P. D. Jones, and P. W. Thorne (2007), Attribution of observed surface humidity changes to human influence, *Nature*, *449*, 710–713, doi:10.1038/nature06207.

Wu, P., R. Wood, and P. A. Stott (2005), Human influence on increasing Arctic river discharges, *Geophys. Res. Lett.*, *32*, L02703, doi:10.1029/2004GL021570.

Zhang, X., K. D. Harvey, W. D. Hogg, and T. R. Yuzyk (2001), Trends in Canadian streamflow, *Water Resour. Res.*, *37*, 987–998, doi:10.1029/2000WR900357.

Zhang, X., F. W. Zwiers, G. C. Hegerl, F. G. Lambert, N. P. Gillett, S. Solomon, P. A. Stott, and T. Nozawa (2007), Detection of human influence on twentieth-century precipitation trends, *Nature*, *448*, 461–465, doi:10.1038/nature06025.

Ziegler, A. D., E. P. Maurer, J. Sheffield, B. Nijssen, E. F. Wood, and D. Lettenmaier (2005), Detection time for plausible changes in annual precipitation, evapotranspiration, and streamflow in three Mississippi River sub-basins, *Clim. Change*, *72*, 17–36, doi:10.1007/s10584-005-5379-4.

H. J. Fowler, Water Resource Systems Research Laboratory, School of Civil Engineering and Geosciences, Cassie Building, Newcastle University, Newcastle upon Tyne NE1 7RU, UK. (h.j.fowler@ncl.ac.uk)

R. L. Wilby, Centre for Hydrological and Ecosystem Science, Department of Geography, Loughborough University, Loughborough LE11 3TU, UK.